

Crystal structure and Hirshfeld surface analysis of 5-hydroxypentanehydrazide

Guilherme Augusto Justen, José Severiano Carneiro Neto, Francielli Sousa Santana, Maria Leiriane Batistel Ribas, Felipe Gomes da Silva de Paula, Priscila Paola Dario and Marcelo Gonçalves Montes D'Oca*

Received 19 February 2024

Accepted 1 April 2024

Departamento de Química, Universidade Federal do Paraná, Centro, Politécnico, Jardim das Américas, 81530-900, Curitiba-PR, Brazil. *Correspondence e-mail: marcelodoca@ufpr.br

Edited by L. Van Meervelt, Katholieke Universiteit Leuven, Belgium

Keywords: hydrazide; lactone; medicinal chemistry; crystal structure; 5-hydroxypentanehydrazide.

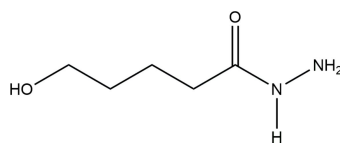
CCDC reference: 2345070

Supporting information: this article has supporting information at journals.iucr.org/e

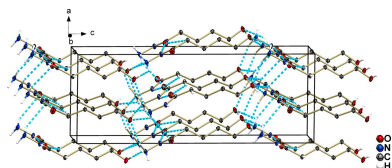
Carboxyhydrazides are widely used in medicinal chemistry because of their medicinal properties and many drugs have been developed containing this functional group. A suitable intermediate to obtain potential hydrazide drug candidates is the title compound 5-hydroxypentanehydrazide, $C_5H_{12}N_2O_2$ (**1**). The aliphatic compound can react both *via* the hydroxyl and hydrazide moieties forming derivatives, which can inhibit Mycobacterium tuberculosis catalase-peroxidase (KatG) and consequently causes death of the pathogen. In this work, the hydrazide was obtained *via* a reaction of a lactone with hydrazine hydrate. The colourless prismatic single crystals belong to the orthorhombic space group $Pca2_1$. Regarding supramolecular interactions, the compound shows classic medium to strong intermolecular hydrogen bonds involving the hydroxyl and hydrazide groups. Besides, the three-dimensional packing also shows weak $H \cdots H$ and $C \cdots H$ contacts, as investigated by Hirshfeld surface analysis (HS) and fingerprint plots (FP).

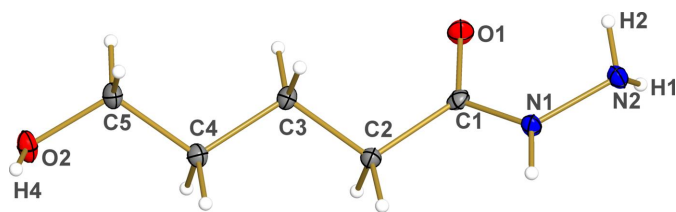
1. Chemical context

Carboxyhydrazides are non-alkaline compounds that can be identified as hydrazines containing an acyl group as one of their substituents, thus they are of general formula $R_1-NR_2-NR_3R_4$, where R_1 is an acyl group and R_2-R_4 are typically hydrogen atoms or alkyl substituents. These compounds, particularly those in which R_2-R_4 are hydrogen atoms, present themselves as valuable functional groups for drug design, since compounds with this functional group and its derivatives tend to have biological activity as antidepressants or antibiotics, for example (Narang *et al.*, 2012). The medicinal potentiality led to the development of several drugs containing this functional group, such as isoniazid, furazolidone, and isocarboxazide (Gegia *et al.*, 2017).



Hydrazides are usually formed *via* the reaction of hydrazine (usually obtained from its hydrochloride or its hydrate) with acyl derivatives such as esters, acyl halides, or anhydrides (Huang *et al.*, 2016). For example, lactones (cyclic esters) promptly react with hydrazine hydrate in a polar solvent such as methanol. In this work, δ -valerolactone was added to hydrazine to afford orthorhombic crystals of 5-hydroxypentanehydrazide **1** (Huang *et al.*, 2016).




Figure 1

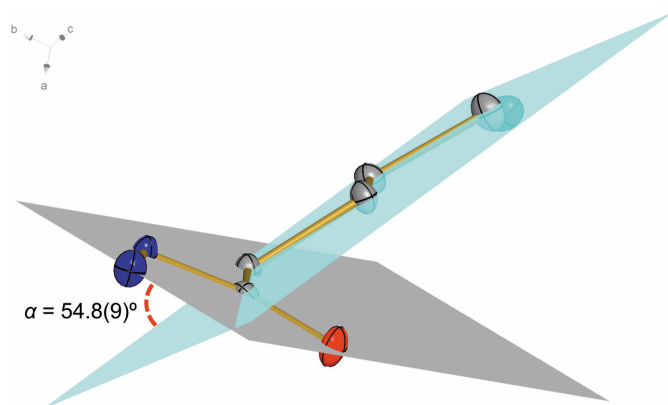
View of the molecular structure of 5-hydroxypentanehydrazide (**1**) with the atom-numbering scheme. Displacement ellipsoids are drawn at the 50% probability level.

Compound **1** was first synthesized by Karakhanov and collaborators in 1969 (Karakhanov *et al.*, 1969). However, this is the first report describing the crystallographic features of 5-hydroxypentanehydrazide.

2. Structural commentary

The molecule of 5-hydroxypentanehydrazide (Fig. 1), crystallizes in the orthorhombic space group $Pca2_1$. The asymmetric unit comprises a unique molecule of **1** with no atoms in special positions, as well as no solvent of crystallization. The C–N, C=O, and N–N bond lengths within the hydrazide group of 1.3376 (17) Å, 1.2375 (16) Å, and 1.4193 (14), respectively, are in agreement with the values reported for aliphatic compounds containing a hydrazide unit (Jensen, 1956; Lo *et al.*, 2020; Kolesnikova *et al.*, 2022). Moreover, the short and unbranched carbon chain formed by atoms C1, C2, C3, C4, and C5, is located in a plane (blue plane in Fig. 2) that makes an angle α of 54.8 (9)° relative to the plane containing the hydrazide atoms N1, N2, C1, C2 and O1 (grey plane in Fig. 2).

The aforementioned conformational features, linked to the orientation of the hydrazide group, are a relatively common characteristic in compounds containing these groups linked to carbon chains. The α angle of 54.8 (9)° observed in compound


Figure 2

Representation of the dihedral angle α formed by the planes containing carbon chain atoms C1, C2, C3, C4, and C5 (blue plane) and the hydrazine group atoms N1, N2, O1, C1, and C2 (grey plane) in **1**. Grey: carbon; red: oxygen; blue: nitrogen. H atoms were omitted for clarity. Displacement ellipsoids are drawn at the 50% probability level.

Table 1

Hydrogen-bond geometry (Å, °).

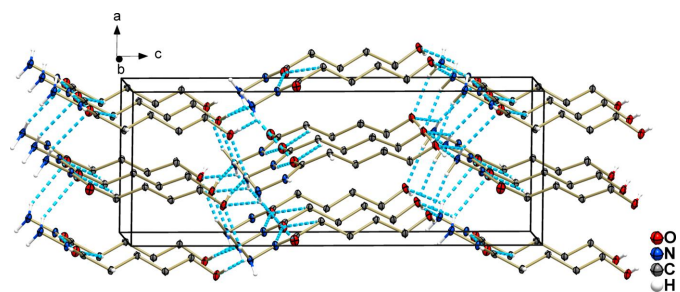
$D-H\cdots A$	$D-H$	$H\cdots A$	$D\cdots A$	$D-H\cdots A$
O2–H4 \cdots N2 ⁱ	0.87 (3)	1.92 (3)	2.7865 (15)	172 (2)
N1–H3 \cdots O1 ⁱⁱ	0.85 (2)	2.03 (2)	2.8662 (14)	166 (2)
N2–H1 \cdots O2 ⁱⁱⁱ	0.91 (2)	2.10 (2)	2.9068 (16)	147.2 (18)
N2–H2 \cdots O1 ^{iv}	0.82 (2)	2.59 (2)	3.2858 (16)	144.0 (16)
N2–H2 \cdots O2 ^v	0.82 (2)	2.57 (2)	3.0789 (14)	122.0 (16)
C2–H2A \cdots O1 ⁱⁱ	0.99	2.57	3.4309 (15)	145

Symmetry codes: (i) $-x + 1, -y + 2, z + \frac{1}{2}$; (ii) $x, y + 1, z$; (iii) $-x + \frac{3}{2}, y, z - \frac{1}{2}$; (iv) $x - \frac{1}{2}, -y + 1, z$; (v) $-x + 1, -y + 1, z - \frac{1}{2}$.

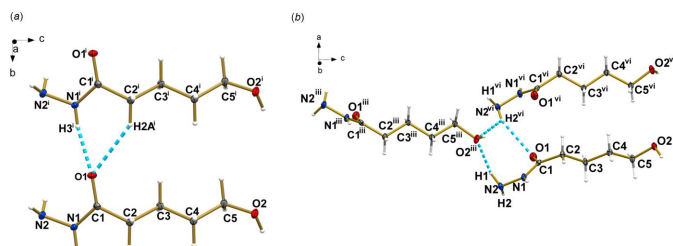
1 is consistent with values reported in the literature, regardless of the carbon chain size. Noteworthy, values include 54.54° for a compound with a twelve-carbon chain (Jensen, 1956), 56.33° for a nine-carbon chain (Jensen & Lingafelter, 1961), and 57.08° for a six-carbon chain (Lee *et al.*, 2016).

3. Supramolecular features

The three-dimensional packing of **1** (Fig. 3) is characterized by several intermolecular O–H \cdots N and N–H \cdots O hydrogen bonds involving the hydroxyl and hydrazine as hydrogen bond donor and acceptor groups (Table 1). Among them, the strongest ones, regarding shortest H \cdots acceptor distances and most linear donor–H \cdots acceptor angles, are the N1–H3 \cdots O1ⁱⁱ [2.03 (2) Å; 166 (2)°; symmetry code: (ii) $x, y + 1, z$] and O2–H4 \cdots N2ⁱ [1.92 (3) Å; 172 (2)°; symmetry code: (i) $-x + 1, -y + 2, z + \frac{1}{2}$], involving the hydrazine and hydroxyl as donor group, respectively, and carbonyl and hydrazine moieties as acceptor groups, respectively. Besides, the hydrazine moiety also promotes hydrogen bonds of medium-force: N2–H1 \cdots O2ⁱⁱⁱ [2.10 (2) Å; 147.2 (18)°; symmetry code: (iii) $-x + \frac{3}{2}, y, z - \frac{1}{2}$], N2–H2 \cdots O1^{iv} [2.59 (2) Å; 144.0 (16)°; symmetry code: (iv) $x - \frac{1}{2}, -y + 1, z$] and N2–H2 \cdots O2^v [2.57 (2) Å; 122.0 (16)°; symmetry code: (v) $-x + 1, 1 - y, z - \frac{1}{2}$]. The latter promotes the formation of chains with a C(9) graph-set motif running in the c -axis direction. A weak hydrogen bond of type C–H \cdots O is also present in the crystal packing. Notably, thanks to this weak interaction, the carbonyl group is the acceptor of a bifurcated hydrogen bond, sharing its electronic density with the C2–H2 and N2–H2 groups and resulting in a six-membered ring with an $R_2^1(6)$ graph-set motif in the b -axis direction (Fig. 4a). The


Figure 3

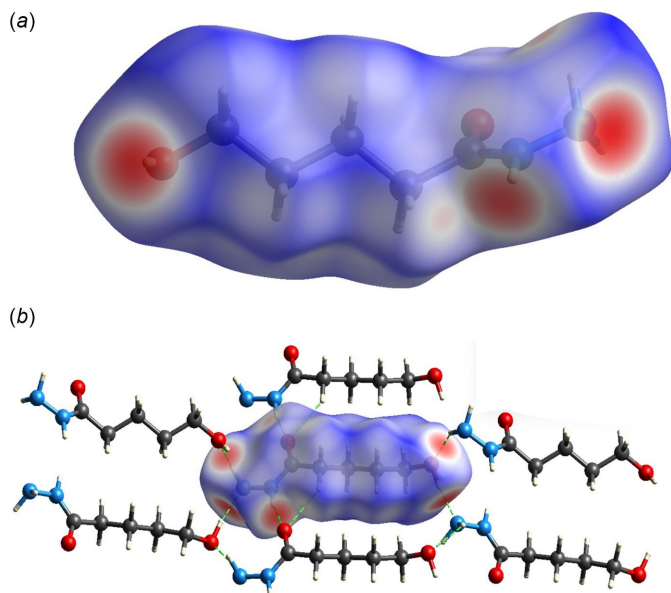
Crystal packing of **1** viewed along the b axis. Intermolecular O–H \cdots N, N–H \cdots O and C–H \cdots O hydrogen bonds are shown as dashed blue lines. H atoms not involved in hydrogen bonding were omitted for clarity.


Figure 4

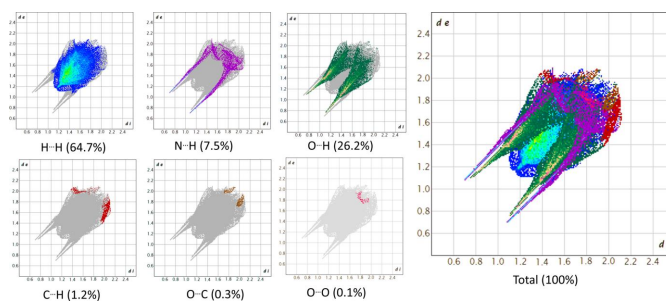
(a) Representation of the six-membered ring formed by N–H \cdots O and C–H \cdots O hydrogen bonds (blue dashed lines) between adjacent molecules in the *b*-axis direction. (b) Representation of the seven-membered ring formed by N–H \cdots O hydrogen bonds (blue dashed lines) between carbonyl and hydrazide groups of adjacent molecules in the *a*-axis direction. Symmetry codes: (i) $x, -y + 1, z$; (iii) $-x + \frac{3}{2}, y, z - 1$; (vi) $x + \frac{1}{2}, -y + 1, z$. Displacement ellipsoids are drawn at the 50% probability level.

formation of seven-membered rings with an $R_2^3(7)$ graph-set motif is observed involving the H1–N2–N1–C1–O1 \cdots H2^{vi} \cdots O2ⁱⁱⁱ moiety in the *a*-axis direction [symmetry code: (iii) $-x + \frac{3}{2}, y, z - \frac{1}{2}$; (vi) $x + \frac{1}{2}, -y + 1, z$; Fig. 4b). Together, these interactions act cooperatively for the stability of **1** in the solid state (Sutor *et al.*, 1962; Domagała & Grabowski, 2005).

The non-covalent interactions responsible for the crystal packing were also investigated by a Hirshfeld surface analysis (HS; Hirshfeld, 1977), performed with *CrystalExplorer 21.5* (Spackman *et al.*, 2021). The Hirshfeld surface provides a three-dimensional representation that elucidates molecular interactions through the mathematical distance functions d_i , denoting the distance from the surface to the nearest atom within it, and d_e , denoting the distance from the surface to the nearest atom outside of it. The normalization of the d_i and d_e distances by the van der Waals radius leads to the d_{norm}


Figure 5

Representation of (a) the Hirshfeld surface for **1** plotted over d_{norm} and (b) illustration of the N–H \cdots O, O–H \cdots N and C–H \cdots O interactions depicted by dashed green lines.


Figure 6

Fingerprint plots for **1** showing the total contribution of individual interactions and those delineated into H \cdots H, N \cdots H/H \cdots N, O \cdots H/H \cdots O, C \cdots H/H \cdots C, O \cdots C/C \cdots O and O \cdots O interactions.

function, which enables the visualization of a surface that delineates regions involved in both accepting and donating intermolecular interactions. A key component of this analysis entails the generation of 2D fingerprint plots (FP), providing two-dimensional representations of the Hirshfeld surface.

Using the d_{norm} function, expressed by a colour scale, this method describes the strength of interatomic interactions. Red and blue indicate interatomic contacts where the distance between atoms is smaller or larger, respectively, than the sum of the van der Waals radii of the atoms involved, while white indicates contacts with distances close to the sum of the van der Waals radii.

In the case of compound **1**, the red colour in Fig. 5a highlights the region of most intense contacts involving the nitrogen, oxygen and hydrogen atoms from the hydrazide and hydroxyl groups with adjacent oxygen atoms. Fig. 5b illustrates the nearest molecules within the crystal packing, delineating the spatial arrangement of the shortest interactions. Meanwhile, blue surfaces, which indicate longer-range interactions, arise mainly from H \cdots H contributions.

Fingerprint plots (FP) were generated to quantify the contribution of each interatomic interaction to the supramolecular structure. For this purpose, the d_i (x axis) and d_e (y axis) distances, expressed in Ångströms, of the HS are used. For **1**, the percentages of the surface area correspond to 64.7% for H \cdots H, 26.2% for O \cdots H/H \cdots O, 7.5% for N \cdots H/H \cdots N, 1.2% for C \cdots H/H \cdots C, 0.3% for O \cdots C/C \cdots O and 0.1% for O \cdots O interactions, as shown in Fig. 6.

4. Database survey

A survey of the Cambridge Structural Database (CSD2023.2.0, version 5.45, November 2023; Groom *et al.*, 2016) revealed several similar structures. 5-Hydroxypentanehydrazide was first synthesized as a byproduct of the reaction of dihydropyran and phenyl azide (Karakhanov *et al.*, 1969) and has never had its structural properties discussed, although it was first obtained in its crystalline form. The synthesis and crystallographic characterization of other similar aliphatic hydrazide derivatives has been reported: *t*-butyl hydrazinecarboxylate (CSD refcode RENZUJ; Aitken & Slawin, 2022), α -cyanoacetohydrazide (CYACHZ; Chieh,

Table 2
Experimental details.

Crystal data	
Chemical formula	C ₅ H ₁₂ N ₂ O ₂
<i>M</i> _r	132.17
Crystal system, space group	Orthorhombic, <i>Pca</i> 2 ₁
Temperature (K)	100
<i>a</i> , <i>b</i> , <i>c</i> (Å)	7.1686 (5), 4.8491 (3), 19.1276 (14)
<i>V</i> (Å ³)	664.90 (8)
<i>Z</i>	4
Radiation type	Mo <i>K</i> α
<i>μ</i> (mm ⁻¹)	0.10
Crystal size (mm)	0.32 × 0.16 × 0.13
Data collection	
Diffractionmeter	Bruker D8 Venture/Photon 100 CMOS
Absorption correction	Multi-scan (<i>SADABS</i> ; Krause <i>et al.</i> , 2015)
<i>T</i> _{min} , <i>T</i> _{max}	0.731, 0.746
No. of measured, independent and observed [<i>I</i> > 2σ(<i>I</i>)] reflections	26421, 1567, 1527
<i>R</i> _{int}	0.029
(sin θ/λ) _{max} (Å ⁻¹)	0.655
Refinement	
<i>R</i> [<i>F</i> ² > 2σ(<i>F</i> ²)], <i>wR</i> (<i>F</i> ²), <i>S</i>	0.022, 0.059, 1.08
No. of reflections	1567
No. of parameters	98
No. of restraints	1
H-atom treatment	H atoms treated by a mixture of independent and constrained refinement
Δρ _{max} , Δρ _{min} (e Å ⁻³)	0.21, -0.19
Absolute structure	Flack <i>x</i> determined using 732 quotients [(<i>I</i> ⁺) - (<i>I</i> ⁻)] / [(<i>I</i> ⁺) + (<i>I</i> ⁻)] (Parsons <i>et al.</i> , 2013)
Absolute structure parameter	-0.1 (2)

Computer programs: *APEX4* (Bruker, 2022), *SAINT* (Bruker, 2019), *SHELXT2015* (Sheldrick, 2015a), *SHELXL2019/2* (Sheldrick, 2015b), *DIAMOND* (Brandenburg & Putz, 1999) and *WinGX* (Farrugia, 2012).

1973), *n*-dodecanoic acid hydrazide (DDEAHN; Jensen, 1956), hexanedihydrazide (MUYRIK; Lo *et al.*, 2020), *n*-nonanoic acid hydrazide (NONACH; Jensen & Lingafelter, 1961) and *n*-octanoic acid hydrazide (ZZZOMM; Jensen & Lingafelter, 1953).

5. Synthesis and crystallization

To a round-bottom flask, δ-valerolactone (100 mg, 0.99 mmol), hydrazine hydrate (200 mg, 4.0 mmol) and 5 mL of methanol were added. The resulting solution was maintained stirring under reflux conditions for 24 h. The solution was then allowed to cool slowly to room temperature. After 20 minutes, a solid started to precipitate in the flask. The solid, which was filtered off and air dried, afforded 115.0 mg of colourless crystals of 5-hydroxypentanehydrazide (**1**) in 88.0% yield. The melting point (375–379 K) was in accordance with literature (Karakhanov *et al.*, 1969).

6. Refinement

Crystal data, data collection and structure refinement details are summarized in Table 2. The hydrogen atoms of the carbon chain were included in idealized positions with C–H distances

set to 0.99 Å and refined using a riding model with *U*_{iso}(H) = 1.2*U*_{eq}(C); the other hydrogen atoms were located in difference-Fourier maps and were refined freely.

Acknowledgements

The authors thank the Conselho Nacional de Desenvolvimento Científico e Tecnológico (CNPq), Edital PROIND 2020/UFPR and Coordenação de Aperfeiçoamento de Pessoal de Nível Superior (CAPES) for fellowships. The author's contributions are as follows. GAJ: methodology, writing – original draft; JSCN: formal analysis, resources; FSS: data curation, visualization; MLBR: validation; FGSP: investigation; PPD: writing, review and editing; MGMD: conceptualization, supervision.

Funding information

Funding for this research was provided by: Coordenação de Aperfeiçoamento de Pessoal de Nível Superior (grant No. 23038.003745/2021-31); Pró-Reitoria de Planejamento, Orçamentos e Finanças - UFPR - PROIND 2020 (grant No. 3527).

References

- Aitken, R. & Slawin, A. (2022). *Molbank*, M1482.
- Brandenburg, K. & Putz, H. (1999). *DIAMOND*. Crystal Impact GbR, Bonn, Germany.
- Bruker (2019). *SAINT*. Bruker AXS Inc., Madison, Wisconsin, USA.
- Bruker (2022). *APEX4*. Bruker AXS Inc., Madison, Wisconsin, USA.
- Chieh, P. (1973). *J. Chem. Soc. Perkin Trans. 2*, pp. 1825–1828.
- Domagała, M. & Grabowski, S. J. (2005). *J. Phys. Chem. A*, **109**, 5683–5688.
- Farrugia, L. J. (2012). *J. Appl. Cryst.* **45**, 849–854.
- Gegia, M., Winters, N., Benedetti, A., van Sooling, D. & Menzies, D. (2017). *Lancet Infect. Dis.* **17**, 223–234.
- Groom, C. R., Bruno, I. J., Lightfoot, M. P. & Ward, S. C. (2016). *Acta Cryst.* **B72**, 171–179.
- Hirshfeld, F. L. (1977). *Theor. Chim. Acta*, **44**, 129–138.
- Huang, Y., Fang, G. & Liu, L. (2016). *Natl. Sci.* **3**, 107–116.
- Jensen, L. (1956). *J. Am. Chem. Soc.* **78**, 3993–3999.
- Jensen, L. H. & Lingafelter, E. C. (1953). *Acta Cryst.* **6**, 300–301.
- Jensen, L. H. & Lingafelter, E. C. (1961). *Acta Cryst.* **14**, 507–520.
- Karakhanov, R., Shekhtman, N. & Zefirov, N. (1969). *Chem. Heterocycl. Compd* **5**, 18.
- Kolesnikova, I., Rykov, A. & Shishkov, I. (2022). *J. Mol. Struct.* **1250**, 139–447.
- Krause, L., Herbst-Irmer, R., Sheldrick, G. M. & Stalke, D. (2015). *J. Appl. Cryst.* **48**, 3–10.
- Lee, S. M., Lo, K. M., Tan, S. L. & Tiekink, E. R. T. (2016). *Acta Cryst.* **E72**, 1390–1395.
- Lo, K. M., Lee, S. M. & Tiekink, E. R. (2020). *Z. Krist. New Cryst. Struct.* **235**, 1257–1258.
- Narang, R., Narasimhan, B. & Sharma, S. (2012). *Curr. Med. Chem.* **19**, 569–612.
- Parsons, S., Flack, H. D. & Wagner, T. (2013). *Acta Cryst.* **B69**, 249–259.
- Sheldrick, G. M. (2015a). *Acta Cryst.* **A71**, 3–8.
- Sheldrick, G. M. (2015b). *Acta Cryst.* **C71**, 3–8.
- Spackman, P. R., Turner, M. J., McKinnon, J. J., Wolff, S. K., Grimwood, D. J., Jayatilaka, D. & Spackman, M. A. (2021). *J. Appl. Cryst.* **54**, 1006–1011.
- Sutor, D. (1962). *Nature*, **195**, 68–69.

supporting information

Acta Cryst. (2024). E80, 459-462 [https://doi.org/10.1107/S2056989024002871]

Crystal structure and Hirshfeld surface analysis of 5-hydroxypentanehydrazide

Guilherme Augusto Justen, José Severiano Carneiro Neto, Francielli Sousa Santana, Maria Leiriane Batistel Ribas, Felipe Gomes da Silva de Paula, Priscila Paola Dario and Marcelo Gonçalves Montes D'Oca

Computing details

5-Hydroxypentanehydrazide

Crystal data

$C_5H_{12}N_2O_2$

$M_r = 132.17$

Orthorhombic, $Pca2_1$

$a = 7.1686$ (5) Å

$b = 4.8491$ (3) Å

$c = 19.1276$ (14) Å

$V = 664.90$ (8) Å³

$Z = 4$

$F(000) = 288$

$D_x = 1.320$ Mg m⁻³

Mo $K\alpha$ radiation, $\lambda = 0.71073$ Å

Cell parameters from 9932 reflections

$\theta = 4.2$ – 28.7°

$\mu = 0.10$ mm⁻¹

$T = 100$ K

Prism, colourless

$0.32 \times 0.16 \times 0.13$ mm

Data collection

Bruker D8 Venture/Photon 100 CMOS diffractometer

Radiation source: fine-focus sealed tube

Detector resolution: 10.4167 pixels mm⁻¹

φ and ω scans

Absorption correction: multi-scan (SADABS; Krause *et al.*, 2015)

$T_{\min} = 0.731$, $T_{\max} = 0.746$

26421 measured reflections

1567 independent reflections

1527 reflections with $I > 2\sigma(I)$

$R_{\text{int}} = 0.029$

$\theta_{\max} = 27.8^\circ$, $\theta_{\min} = 4.3^\circ$

$h = -9 \rightarrow 9$

$k = -6 \rightarrow 6$

$l = -25 \rightarrow 25$

Refinement

Refinement on F^2

Least-squares matrix: full

$R[F^2 > 2\sigma(F^2)] = 0.022$

$wR(F^2) = 0.059$

$S = 1.08$

1567 reflections

98 parameters

1 restraint

Primary atom site location: dual

Secondary atom site location: difference Fourier map

Hydrogen site location: mixed

H atoms treated by a mixture of independent and constrained refinement

$w = 1/[\sigma^2(F_o^2) + (0.0379P)^2 + 0.0769P]$

where $P = (F_o^2 + 2F_c^2)/3$

$(\Delta/\sigma)_{\max} < 0.001$

$\Delta\rho_{\max} = 0.21$ e Å⁻³

$\Delta\rho_{\min} = -0.19$ e Å⁻³

Absolute structure: Flack x determined using

732 quotients $[(I^-)-(I)]/[(I^+)+(I)]$ (Parsons *et al.*, 2013)

Absolute structure parameter: -0.1 (2)

Special details

Geometry. All esds (except the esd in the dihedral angle between two l.s. planes) are estimated using the full covariance matrix. The cell esds are taken into account individually in the estimation of esds in distances, angles and torsion angles; correlations between esds in cell parameters are only used when they are defined by crystal symmetry. An approximate (isotropic) treatment of cell esds is used for estimating esds involving l.s. planes.

Fractional atomic coordinates and isotropic or equivalent isotropic displacement parameters (\AA^2)

	<i>x</i>	<i>y</i>	<i>z</i>	$U_{\text{iso}}^*/U_{\text{eq}}$
O1	0.58285 (13)	0.44491 (18)	0.38116 (6)	0.0149 (2)
O2	0.71437 (14)	0.7429 (2)	0.71584 (5)	0.0151 (2)
N1	0.51145 (15)	0.8787 (2)	0.34743 (5)	0.0105 (2)
N2	0.42516 (17)	0.7936 (2)	0.28423 (6)	0.0122 (2)
C1	0.58629 (18)	0.6966 (3)	0.39182 (6)	0.0097 (2)
C3	0.58864 (17)	0.6955 (2)	0.52353 (6)	0.0110 (2)
H3A	0.453999	0.740443	0.525239	0.013*
H3B	0.601004	0.492251	0.522213	0.013*
C4	0.68313 (18)	0.8053 (3)	0.58941 (6)	0.0115 (3)
H4A	0.818747	0.768536	0.586516	0.014*
H4B	0.665552	1.007624	0.591765	0.014*
C5	0.60650 (19)	0.6753 (3)	0.65582 (7)	0.0139 (3)
H5A	0.476648	0.738769	0.663034	0.017*
H5B	0.603920	0.472447	0.650158	0.017*
C2	0.67320 (18)	0.8176 (2)	0.45691 (6)	0.0106 (2)
H2A	0.654542	1.019919	0.456926	0.013*
H2B	0.809132	0.781623	0.456417	0.013*
H1	0.514 (3)	0.715 (4)	0.2573 (12)	0.024 (5)*
H2	0.345 (3)	0.680 (4)	0.2935 (10)	0.016 (4)*
H3	0.517 (3)	1.052 (4)	0.3531 (11)	0.020 (5)*
H4	0.664 (4)	0.890 (5)	0.7337 (13)	0.034 (6)*

Atomic displacement parameters (\AA^2)

	U^{11}	U^{22}	U^{33}	U^{12}	U^{13}	U^{23}
O1	0.0227 (5)	0.0074 (4)	0.0146 (4)	0.0001 (3)	-0.0016 (4)	-0.0006 (3)
O2	0.0204 (5)	0.0158 (4)	0.0092 (4)	0.0034 (4)	-0.0026 (4)	-0.0033 (4)
N1	0.0161 (5)	0.0070 (5)	0.0084 (5)	-0.0001 (4)	-0.0012 (4)	-0.0011 (4)
N2	0.0160 (5)	0.0111 (5)	0.0094 (5)	-0.0012 (4)	-0.0029 (4)	-0.0016 (4)
C1	0.0106 (5)	0.0096 (5)	0.0090 (6)	-0.0006 (4)	0.0033 (4)	0.0005 (4)
C3	0.0127 (5)	0.0120 (5)	0.0082 (5)	-0.0013 (4)	0.0005 (4)	0.0012 (5)
C4	0.0132 (6)	0.0120 (6)	0.0092 (5)	-0.0010 (4)	0.0003 (5)	-0.0009 (5)
C5	0.0170 (6)	0.0166 (6)	0.0081 (5)	-0.0031 (5)	-0.0008 (5)	-0.0007 (5)
C2	0.0136 (6)	0.0093 (5)	0.0088 (5)	-0.0014 (5)	-0.0004 (5)	0.0002 (4)

Geometric parameters (\AA , $^\circ$)

O1—C1	1.2375 (16)	C3—C2	1.5303 (16)
O2—C5	1.4223 (16)	C3—H3A	0.9900

O2—H4	0.87 (3)	C3—H3B	0.9900
N1—C1	1.3376 (17)	C4—C5	1.5208 (17)
N1—N2	1.4193 (14)	C4—H4A	0.9900
N1—H3	0.85 (2)	C4—H4B	0.9900
N2—H1	0.91 (2)	C5—H5A	0.9900
N2—H2	0.82 (2)	C5—H5B	0.9900
C1—C2	1.5109 (16)	C2—H2A	0.9900
C3—C4	1.5265 (16)	C2—H2B	0.9900
C5—O2—H4	106.4 (17)	C5—C4—H4A	109.1
C1—N1—N2	121.55 (11)	C3—C4—H4A	109.1
C1—N1—H3	123.8 (15)	C5—C4—H4B	109.1
N2—N1—H3	114.6 (15)	C3—C4—H4B	109.1
N1—N2—H1	107.3 (14)	H4A—C4—H4B	107.8
N1—N2—H2	108.6 (13)	O2—C5—C4	112.48 (10)
H1—N2—H2	109.6 (19)	O2—C5—H5A	109.1
O1—C1—N1	122.60 (12)	C4—C5—H5A	109.1
O1—C1—C2	121.81 (11)	O2—C5—H5B	109.1
N1—C1—C2	115.58 (11)	C4—C5—H5B	109.1
C4—C3—C2	112.13 (10)	H5A—C5—H5B	107.8
C4—C3—H3A	109.2	C1—C2—C3	111.87 (10)
C2—C3—H3A	109.2	C1—C2—H2A	109.2
C4—C3—H3B	109.2	C3—C2—H2A	109.2
C2—C3—H3B	109.2	C1—C2—H2B	109.2
H3A—C3—H3B	107.9	C3—C2—H2B	109.2
C5—C4—C3	112.62 (10)	H2A—C2—H2B	107.9
N2—N1—C1—O1	-0.98 (19)	O1—C1—C2—C3	-55.33 (16)
N2—N1—C1—C2	180.00 (11)	N1—C1—C2—C3	123.70 (11)
C2—C3—C4—C5	-177.29 (11)	C4—C3—C2—C1	176.88 (10)
C3—C4—C5—O2	170.30 (10)		

Hydrogen-bond geometry (\AA , $^\circ$)

$D-H\cdots A$	$D-H$	$H\cdots A$	$D\cdots A$	$D-H\cdots A$
O2—H4 \cdots N2 ⁱ	0.87 (3)	1.92 (3)	2.7865 (15)	172 (2)
N1—H3 \cdots O1 ⁱⁱ	0.85 (2)	2.03 (2)	2.8662 (14)	166 (2)
N2—H1 \cdots O2 ⁱⁱⁱ	0.91 (2)	2.10 (2)	2.9068 (16)	147.2 (18)
N2—H2 \cdots O1 ^{iv}	0.82 (2)	2.59 (2)	3.2858 (16)	144.0 (16)
N2—H2 \cdots O2 ^v	0.82 (2)	2.57 (2)	3.0789 (14)	122.0 (16)
C2—H2A \cdots O1 ⁱⁱ	0.99	2.57	3.4309 (15)	145

Symmetry codes: (i) $-x+1, -y+2, z+1/2$; (ii) $x, y+1, z$; (iii) $-x+3/2, y, z-1/2$; (iv) $x-1/2, -y+1, z$; (v) $-x+1, -y+1, z-1/2$.